Assembly of Lipoprotein Particles Containing Apolipoprotein-B: Structural Model for the Nascent Lipoprotein Particle

Paul E. Richardson,*§ Medha Manchekar,† Nassrin Dashti,† Martin K. Jones,† Anne Beigneux,‡ Stephen G. Young,‡ Stephen C. Harvey,§ and Jere P. Segrest†

*Department of Biochemistry and Molecular Genetics, and †Department of Medicine, Atherosclerosis Research Unit, University of Alabama at Birmingham Medical Center, Birmingham, Alabama; ‡Gladstone Institute of Cardiovascular Disease, University of California at San Francisco, San Francisco, California; and §School of Biology, Georgia Institute of Technology, Atlanta, Georgia

ABSTRACT Apolipoprotein B (apoB) is the major protein component of large lipoprotein particles that transport lipids and cholesterol. We have developed a detailed model of the first 1000 residues of apoB using standard sequence alignment programs (ClustalW and MACAW) and the MODELLER6 package for three-dimensional homology modeling. The validity of the apoB model was supported by conservation of disulfide bonds, location of all proline residues in turns and loops, and conservation of the hydrophobic faces of the two C-terminal amphipathic β-sheets, βA (residues 600–763) and βB (residues 780–1000). This model suggests a lipid-pocket mechanism for initiation of lipoprotein particle assembly. In a previous model we suggested that microsomal triglyceride transfer protein might play a structural role in completion of the lipid pocket. We no longer think this likely, but instead propose a hairpin-bridge mechanism for lipid pocket completion. Salt-bridges between four tandem charged residues (717–720) in the turn of the hairpin-bridge and four tandem complementary residues (997–1000) at the C-terminus of the model lock the bridge in the closed position, enabling the deposition of an asymmetric bilayer within the lipid pocket.

INTRODUCTION

Apolipoproteins are responsible for the transport of lipids and cholesterol. Apolipoprotein B (apoB) is a non-exchangeable lipoprotein and exists in two forms in humans, apoB-100 and apoB-48. ApoB-100 is the full-length protein, consisting of 4536 amino acid residues. ApoB-48 is the truncated form of apoB-100 (consisting of amino acid residues 1–2152) and is produced by the introduction of a premature stop codon in the mRNA sequence by alternative mRNA splicing by the APOBEC-1 complex (Chen et al., 1987; Greeve et al., 1991). ApoB-48 is synthesized in the intestine and is essential for the formation and secretion of chylomicrons. ApoB-100 is synthesized in the liver and is an essential structural component of very low density lipoprotein, intermediate-density lipoprotein, and low-density lipoprotein. ApoB-100 also serves as a ligand for receptor-mediated uptake of low-density lipoprotein (LDL) by a variety of cells (Law and Scott, 1990; Schumaker et al., 1994; Welty et al., 1995). Deficiency in apoB secretion is accompanied by lack of very low density lipoprotein and chylomicron production, leading to malabsorption of fats and fat-soluble vitamins (Linton et al., 1993; Sharp et al., 1993; Shoulders et al., 1993). High plasma levels of LDL-cholesterol and apoB are risk factors for atherosclerosis, a leading cause of death in western countries (Sniderman et al., 1980; Tyroler, 1987).

Because of its high insolubility in an aqueous environment, apoB is irreversibly associated with the lipoprotein particle and is never found free in the plasma. This insolubility has made determining the structure of apoB difficult. Experimental evidence and theoretical predictions have offered insights into the structure of apoB and the apoB lipoprotein particles. Early work using calorimetry and x-ray diffraction (Atkinson et al., 1977; Deckelbaum et al., 1977, 1975; Muller et al., 1978), and more recently cryo-electron microscopy (Chatterton et al., 1995a,b, 1991; Gantz et al., 2000; Spin and Atkinson, 1995; van Antwerpen et al., 1997, 1999), indicated that apoB is located on the surface of a spheroidal lipoprotein particle.

Computer analysis with the program LOCATE led to the currently accepted pentapartite model (NH_2-$\beta\alpha_1$-β_1-α_2-β_2-α_3-COOH) for apoB-100 in which domains rich in amphipathic β-sheets alternate with those rich in amphipathic α-helices (Segrest et al., 1994). LOCATE examines the protein sequence to predict the location of amphipathic α-helices if patterns of hydrophilic and hydrophobic residues repeat with a period of $\sim$3.6 residues; and amphipathic β-strands for patterns of alternating hydrophilic and hydrophobic residues. These results were valuable in getting an overall idea of the topology and domains of apoB-100, but did not provide data that could produce a detailed structural model for apoB.

Sequence analyses and intron/exon boundary identification of apoB have indicated that the N-terminal $\beta\alpha_1$-domain is homologous to the lipovitellins (Baker, 1988; Shoulders et al., 1994). Lipovitellins are major lipid transport proteins of egg laying species, transporting lipids from the liver to the oocytes. The crystal structure of silver lamprey lipovitellin has been determined at 2.8 Å resolution and reveals a β-barrel

Submitted May 21, 2004, and accepted for publication October 19, 2004.

Address reprint requests to Jere P. Segrest, Tel.: 205-934-4420; Fax: 205-975-8079; E-mail: segrest@uab.edu.

0006-3495/05/04/2789/12 $2.00

doi: 10.1529/biophysj.104.046235

structure (βC-region) sitting on top of a triangular-shaped cavity (Raag et al., 1988; Sharrock et al., 1992). The cavity is bounded by three β-sheets (βA, βB, βD) that were proposed to accommodate lipids within the cavity or lipid pocket; two partially resolved lipids were associated with the β-barrel in the crystal structure (Raag et al., 1988; Sharrock et al., 1992). The βA- and βB-sheets form two sides of the pocket, whereas the βD-sheet forms the base, leaving two triangular-shaped openings at either end of the pocket. An 11-stranded, partially closed β-barrel (βC) is found at the N-terminal end. Surrounding the smallest open end of the triangular βA/βB/βD cavity is a belt formed by17 antiparallel α-helices that are stacked in a double layer.

ApoB sequence homology to lipovitellin allowed a structural model for the N-terminal 587 residues of apoB to be generated using the crystal structure of silver lamprey lipovitellin (Mann et al., 1999). This model offered valuable insight into the βC-domain and the α-helical domain (1–587) of apoB, but since it did not extend into the lipid-binding pocket of lipovitellin (587–1529), it did not offer insights into the mechanism for initial assembly of the lipid components of apoB-containing lipoprotein particles.

Further sequence analysis has suggested that the homology of lipovitellin and apoB extends beyond the first 587 amino acids, to include the first 1000 amino acid residues of apoB (Segrest et al., 1999), a region that includes the βA- and βB-domains of lipovitellin. Because this region is homologous to the proposed lipid binding cavity in lipovitellin, it was proposed that this region might be a lipid-binding pocket for apoB (Segrest et al., 1999). Since the homology of apoB did not extend to the βD-sheet in lipovitellin, it was suggested on the basis of the presence of a pronounced cluster of amphipathic β-strands identified by LOCATE that microsomal triglyceride transfer protein (MTP) might function as the βD-domain, closing the base of the lipid pocket (Segrest et al., 2001). MTP has been proposed to act as a lipid transfer protein (Du et al., 1996; Wetterau et al., 1997) and is apparently required for the secretion of apoB-containing particles. Further, MTP may have more than one function (Herscovitz et al., 1991).

In this article we report further studies on the homology of the first 1000 amino acids of apoB to the lipovitellins using local sequence homology search methods to expand the sequence identity/similarity between apoB and lipovitellin. These results have located conserved blocks of sequences beyond the first 600 residues in apoB. Sequence comparison using the program LOCATE has identified conserved amphipathic β-strands in human apoB and mouse apoB. From these analyses we have created a structural model of the first 1000 residues of apoB (the $\beta\alpha_1$-domain). This model provides further insights into the proposed lipid-binding pocket of apoB, identifies the domains that are responsible for lipid association, and suggests the possible mechanism by which apoB adjusts its structure to initiate particle assembly and accommodate lipid particle expansion.

MATERIALS AND METHODS

Sequence and model accession numbers

Human apoB (accession number LPHUB), mouse apoB (XP_137955), lamprey vitellogenin (AAA49327), chicken vitellogenin (P87498), sturgeon vitellogenin (Q90243), frog vitellogenin (P18709), tilapia vitellogenin (T31095), trout vitellogenin (JC4956), and killifish vitellogenin (Q90508) sequences are available at the NCBI database. Rabbit and lemur apoB sequences were obtained from the genomic DNA sequences deposited in the Berkeley PGA, an NHLBI-supported Program for Genomics Applications. The accession number for lamprey lipovitellin is 1LLV and can be found in the Protein DataBank.

Database searches and alignments

The first 1000 residues of apoB were used to identify homologous proteins using the web-based BLASTp program from the National Centre for Biotechnology (Altschul et al., 1990). The default settings were used for the BLASTp search. The most significant matches to human apoB belonged to rat, opossum, and pig apoB proteins, along with a multitude of vitellogenin proteins from a wide range of species including silver lamprey lipovitellin.

The alignment program ClustalW (Thompson et al., 1994) was used to align silver lamprey lipovitellin (residues 1–1074) and apoB (residues 1–1000) giving a global alignment for the two sequences. The program MACAW (Schuler et al., 1991) was used to identify local sequence homology in the first 1000 amino acid sequences of mouse and human apoB and the first 1100 amino acid sequences of lamprey, frog, and chicken lipovitellins. The program LOCATE (Segrest et al., 1994) was then used to identify potential amphipathic β-strands in the first 1000 amino acids of both mouse and human apoB. The final alignment was a merging of the ClustalW (1–620) and MACAW alignments (621–1000), with the LOCATE analysis being used as a guide in aligning regions 600–1000 in apoB.

Modeling

The final alignment was used to generate the structural model of the first 1000 amino acids of human apoB using the program MODELLER6 (Sali and Blundell, 1993). To eliminate serious steric problems, and to optimize bond lengths and angles, the model was subject to 250 steps of steepest descent energy minimization using the DISCOVER program package from INSIGHT2 (Accelerys, San Diego, CA). Graphical representation of the model was created by RIBBONS (Carson, 1991). Distance measurements were done using both INSIGHT2 and RASMOL (Sayle and Milner-White, 1995). The generation of the helix-turn-helix motif model was done using MODELLER6 and INSIGHT2, and was used to orient the helix-turn-helix flap into the model and correct steric problems.

Truncation and lipid content analysis

Expression plasmids encoding C-terminally truncated forms of apoB-100, i.e., apoB-20.5, apoB-22.0, and apoB-26.5 (1–931, 1–1000, and 1–1200, respectively, of the mature protein lacking the signal peptide) were constructed as previously described in detail (Dashti et al., 2002). Clonal stable transformants of rat hepatoma McA-RH7777 cells expressing above truncated forms of apoB-100 were generated as previously described (Dashti et al., 2002).

Cells were incubated for 24 h in serum-free Dulbecco's modified Eagle's medium (DMEM) containing 0.4 mM of unlabeled or [^{14}C]-labeled oleic acid bound to 0.75% bovine serum albumin (BSA) as previously described (Dashti et al., 2002). The unlabeled conditioned medium was concentrated 10-fold and subjected to density gradient ultracentrifugation as previously described. Forty fractions of 1.0 ml each were collected from the bottom of the centrifuge tube, their densities were measured, and they were analyzed

by 4–20% nondenaturing gradient gel electrophoresis and Western blotting as previously described (Dashti et al., 2002). In metabolically labeled cells, conditioned medium was concentrated 10-fold and applied to 4–20% nondenaturing gradient gel electrophoresis. The gels were dried and subjected to autoradiography and analyzed by computer-assisted densitometry using Labsystem (Helsinki, Finland).

RESULTS

ApoB homology over the first 1000 residues

The complete sequences of human apoB-100 and silver lamprey lipovitellin were aligned using ClustalW (alignment not shown). This alignment indicated that the homology between these two proteins was located in the first 1000 residues of apoB. The first 1000 residues of human apoB were entered into the homology search program BLASTp to identify homologous sequences. The sequence for the first 1000 residues of apoB was compared against all other sequences in the database and the most statistically significant hits were determined. A summary of the results is displayed in Table 1 and shows that the most significant hits are to those of apoB from opossum, pig, and rat. Also included in this list are the vitellogenin proteins from a multitude of different species, including silver lamprey lipovitellin, whose crystal structure with bound lipids has been recently determined (Raag et al., 1988; Sharrock et al., 1992; Thompson and Banaszak, 2002).

Generation of the alignment

A homology search was done using BLASTp (Table 1), the results of which indicated that the first 1000 residues of human apoB are homologous to the first 1075 amino acids of lamprey lipovitellin. Two alignment programs, ClustalW and MACAW, were employed in order to create the best alignment possible. ClustalW (default settings) provides an alignment over entire sequences of apoB and lipovitellin. The alignment was highly conserved over the first 620 residues of apoB, but was not as conserved beyond that point. This is where the MACAW analysis was pivotal. MACAW determines blocks of locally conserved regions between sequences with homology gaps.

TABLE 1 HOMOLOGOUS PROTEINS

Accession#	Animal	Protein	*E*-value
AAH38263	Mouse	ApolipoproteinB	e-0
A27001	Rat	ApolipoproteinB	e-0
BAA86052	Opossum	ApolipoproteinB	e-164
JT0382	Pig	ApolipoproteinB	2e-95
AAG17936	*Chrex*	Vitellogenin	2e-34
BAB69831	Giant prawn	Vitellogenin	1e-26
BAB01568	*Marsupenaeus*	Vitellogenin	2e-23
AAL12620	*Penaeus*	Vitellin	3e-21
P18709	African frog	Vitellogenin A2	4e-16
AAD23878	Fathead minnow	Vitellogenin	2e-14
Q90243	White sturgeon	Vitellogenin	3e-14
Q91062	Silver lamprey	Vitellogenin	2e-12
AAL01527	*Larus*	Vitellogenin	2e-12
NP_739573	Zebra fish	Vitellogenin	4e-12
AAL07472	Carp	Vitellogenin	1e-11
P02845	Chicken	Vitellogenin	1e-10
AAK15157	Haddock	Vitellogenin	2e-10
T31095	Oreochromis	Vitellogenin	3e-9
JC4956	Rainbow trout	Vitellogenin	3e-8

The first 1000 residues of human Apolipoprotein B-100 were entered into the homology search program BLASTp (http://www.ncbi.nlm.nih.gov/blast/) and the most significant homologous proteins were listed. The default settings were used for the web-based search. Italicized names are given (*Genus*) when the common names were not provided in the database.

Both alignments (MACAW and ClustalW) were identical over the first 620 amino acids of apoB (Fig. 1 *A*). The MACAW alignment identified a set of 10 local domains with significant sequence similarity between human apoB and lipovitellin (data not shown); five of these homologous domains were located between residues 620 and 1000 (Fig. 1 *B*). To optimize the alignment and examine the functional properties of the sequence between residues 600 and 1000 in the human apoB sequence, an analysis was done to predict amphipathic β-stranded domains using LOCATE. The first 1000 residues of mouse and human apoB were analyzed by LOCATE (data not shown) and 17 amphipathic β-strands possessing significant lipid affinity were determined (Fig. 1 *C*).

To optimize the alignment between residues 621 and 1000, the homologous domains determined by MACAW were held fixed. By orienting the hydrophobic faces of the amphipathic β-strands toward the lipid pocket interior, the LOCATE analysis for amphipathic β-strands was used to optimize those regions between the conserved domains. Between residues 621 and 1000 we detected 18.6% identity and 40.4% similarity to the lamprey lipovitellin sequence; between residues 1 and 1000 (Fig. 2) apoB had 20.1% identity and 39.6% similarity to lipovitellin (residues 1–1074). These numbers for identity and similarity are similar to those achieved by Mann and co-workers for their apoB model that contained only residues 1–587 (Mann et al., 1999). Although these numbers are low, they should provide a useful low-resolution model.

The apoB-1000 ($\beta\alpha_1$-domain) model

Using the alignment generated and the crystal structure of silver lamprey lipovitellin, a model of the first 1000 residues of apoB was created using the modeling program MODELLER6. The model was optimized with 250 steps of energy minimization to correct any unfavorable angles, bonds, and nonbonded contacts.

The overall topology of the model (Fig. 3, *A* and *B*) shows three unique structural domains in the first 1000 residues (β-barrel, α-helical bundle, and two β-sheets). The conformation of residues 1–587 appears to be similar to the homology model previously generated (Mann et al., 1999). The first 267 residues make up a 10-stranded β-barrel that is not completely enclosed. Inside this partially closed barrel is

A

```
ApoB  EEEMLENVSLVCPKDATRFKHLRKYTYNYEAESSSGVPGTADSRSATRINCKVELEVPQL 60
Lipo  -MWKLLLVALAFALADAQFQPGKVYRYSYDAFSISGLPEPGVNRAGLSGEMKIEIHGHTH 59
          *  *:*. .   ::*:  : * *.*:* * **:* .. .*:.   : *:*:.

ApoB  CSFILKTSQCTLKEVYGFNPEGKALLKKTKNSEEFAAAMSRYELKLAIPEGKQVFLYPEK 120
Lipo  NQATLKITQVNLKYFLGPWP-SDSFYPLTAGYDHFIQQL-EVPVRFDYSAGRIGDIYAPP 117
       .  ** :* .** . *  * ..::   * . :.*   : .  :::  . *:   :*.

ApoB  DEPTYILNIKRGIISALLVPPETEEAKQVLFLDTVYGNCSTHFTVKTRKGNVATEISTER 180
Lipo  QVTDTAVNIVRGILNLFQLSLKKNQQTFELQETGVEGICQTTYVVQEGYRTNEMAVVKTK 177
      : .   :** ***:. : :. :.:: .  *    * * *.* :.*:    .    : . :

ApoB  DLGQCDRFKPIRTGISPLALIKGMTRPLSTLISSSQSCQYTLDAKRKHVAEAICKEQHLF 240
Lipo  DLNNCDHKVYKTMGTAYAERCPTCQKMNKNLRSTAVYNYAIFDEPSGYIIKSAHSEEIQQ 237
      **.:**:      * :          :  ..* *::      :*    :: ::  .*:

ApoB  LPFSYKNKYGMVAQVTQTLKLEDTPKINSRFFGEGTKKMG--------------LAFEST 286
Lipo  LSVFDIKEGNVVIESRQKLILEGIQSAPAASQAASLQNRGGLMYKFPSSAITKMSSLFVT 297
      *..   :: .:* :  *.* **.  .  :   . . :: *                ::  *

ApoB  KSTSPPKQAEAVLKTLQELKKLTISEQNIQRANLFNKLVTELRGLSDEAVTSLLPQLIEV 346
Lipo  KGKNLESEIHTVLKHLVENNQLSVHED---APAKFLRLTAFLRNVDAGVLQSIWHKLHQQ 354
      *...  .: .:*** * * ::*:: *:    .  * :*.: **.:.  .: *:  :* :

ApoB  SSPITLQALVQCGQPQCSTHILQWLKRVHANPLLIDVVTYLVALIPEPSAQQLREIFNMA 406
Lipo  KD--YRRWILDAVPAMATSEALLFLKRTLASEQLTSAEATQIVYSTLSNQQATRESLSYA 412
      ..    : :::.  . .::. * :***. *.  * .. :  :.  . .. *  ** :. *
```

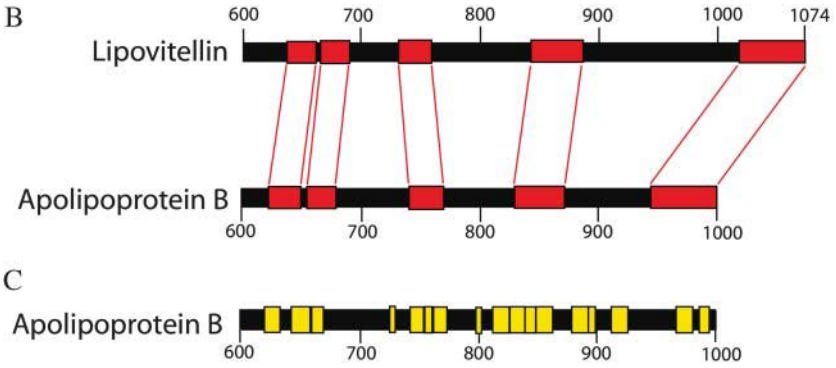

FIGURE 1 Alignment and analysis of apoB-22.5. (*A*) Sequence alignment for the first 620 amino acids of human apoB and the homologous residues in lipovitellin. (*B*) The red boxes represent local sequence homology between apoB and lipovitellin that were recognized using the alignment program MACAW. (*C*) The yellow boxes are conserved regions in mouse and human apoB sequence that the program LOCATE identified as potential amphipathic β-strands.

an amphipathic α-helix. There is a large undefined loop (residues 268–300) that connects the β-barrel to a series of 17 α-helices.

The α-helical domain extends from residues 300–600 and is arranged in a double-layered antiparallel picket fence arrangement on the outside faces of the βA- and βB-sheets. This domain surrounds most of the βA-sheets (residues 600–763) and part of the βB-sheet (residues 780–1000), holding them in place. The βA- and βB-sheets are arranged like two sides of a three-sided pyramid, with a large opening at the base (Fig. 3 *A*) and a smaller opening at the apex where the α-helical domain is located (Fig. 3 *B*). Without the third side that is provided in lipovitellin by the βD-sheet, this arrangement of sheets creates a large asymmetric V-shaped hydrophobic cavity in the structure. There is a small loop-helix at the apex of the two-sided pyramid (residues 764–779) that connects the two β-sheets. There is a large undefined loop joining two adjacent strands in the βA-sheet (residues 666–746) that is not homologous to any sequence in lipovitellin or any other sequence in the Genbank database (data not shown). Since no structures were homologous for the modeling of this loop, it was not included in Fig. 3.

Analysis of the apoB:1000 model

The program PROCHECK (Laskowski et al., 1993) was used to check the geometry and steric contacts of the model and it showed that the homology model was reasonable with 97.9% of the residues in the allowed regions of the Ramachandran plot (data not shown). The vast majority of those residues outside the allowed regions were located in loops, not in secondary structures.

Disulfide bonds

Of the eight disulfide bonds determined in apoB, seven of them are located in the first 1000 residues (Yang et al., 1990). Analysis of the model indicates that all of the seven disulfide bonds are correctly paired and within 6 Å of one another. The model was created without manipulation or intervention on our part, so this is very strong support for the model. The

```
Lipo  -MWKLLLVALAFALADAQFQPGKVYRYSYDAFSISGLPEPGVNRAGLSGEMKIEIHGHTH    59
ApoB  EEEMLENVSLVCPKDATRFKHLRKYTYNYEAESSSGVPGTADSRSATRINCKVELEVPQL    60

Lipo  NQATLKITQVNLKYFLGPWP-SDSFYPLTAGYDHFIQQL-EVPVRFDYSAGRIGDIYAPP   117
ApoB  CSFILKTSQCTLKEVYGFNPEGKALLKKTKNSEEFAAAMSRYELKLAIPEGKQVFLYPEK   120

Lipo  QVTDTAVNIVRGILNLFQLSLKKNQQTFELQETGVEGICQTTYVVQEGYRTNEMAVVKTK   177
ApoB  DEPTYILNIKRGIISALLVPPETEEAKQVLFLDTVYGNCSTHFTVKTRKGNVATEISTER   180

Lipo  DLNNCDHKVYKTMGTAYAERCPTCQKMNKNLRSTAVYNYAIFDEPSGYIIKSAHSEEIQQ   237
ApoB  DLGQCDRFKPIRTGISPLALIKGMTRPLSTLISSSQSCQYTLDAKRKHVAEAICKEQHLF   240

Lipo  LSVFDIKEGNVVIESRQKLILEGIQSAPAASQAASLQNRGGLMYKFPSSAITKMSSLFVT   297
ApoB  LPFSYKNKYGMVAQVTQTLKLEDTPKINSRFFGEGTKKMG-------------LAFEST   286

Lipo  KGKNLESEIHTVLKHLVENNQLSVHED---APAKFLRLTAFLRNVDAGVLQSIWHKLHQQ   354
ApoB  KSTSPPKQAEAVLKTLQELKKLTISEQNIQRANLFNKLVTELRGLSDEAVTSLLPQLIEV   346

Lipo  KD--YRRWILDAVPAMATSEALLFLKRTLASEQLTSAEATQIVYSTLSNQQATRESLSYA   412
ApoB  SSPITLQALVQCGQPQCSTHILQWLKRVHANPLLIDVVTYLVALIPEPSAQQLREIFNMA   406

Lipo  RELLHTSFIRNRPILRKTAVLGYGSLVFRYCANTVSCPDELLQPLHDLLSQSSD--RADE   470
ApoB  RDQRS-----------RATLYALSHAVNNYHKTNPTGTQELLDIANYLMEQIQDDCTGDE   455

Lipo  EEIVLALKALGNAGQ-PNSIKKIQRFLPGQGKSLDEYSTRVQAEAIMALRNIAKRDPRKV   529
ApoB  DYTYLILRVIGNMGQTMEQLTPELKSSILKCVQSTKPSLMIQKAAIQALRKMEPKD--KD   513

Lipo  QEIVLPIFLNVAIKSELRIRSCIVFFESKPSVALVSMVAVRLRREPNLQVASFVYSQMRS   589
ApoB  QEVLLQTFLDDASPGDKRLAAYLMLMRS-PSQADINKIVQILPWEQNEQVKNFVASHIAN   572

Lipo  LSRSSNPEFRDVAAACSVAIKMLGSKLDRLGCRYSKAVHVDTFNARTM-----AGVSADY   644
ApoB  ILNSEELDIQDLKKLVKEVLKES--QLPTVMDFRKFSRNYQLYKSVSLPSLDPASAKIEG   630

Lipo  FRINSPSGPLPRAVAAKIRGQGMGYAS-DIVEFGLRAEGLQELLY-----RG----SQEQ   694
ApoB  NLIFDPNNYLPKESMLKTTLTAFGFASADLIEIGLEGKGFEPTLEALFGKQGFFPDSVNK   690

Lipo  DAY---GTALD--RQTLLRS-G---QARSHVSSIHDTLRKLSD-WKSVP-EERPLASGYV   743
ApoB  ALYWVNGQVPDGVSKVLVDHFGYTKDDKHEQDMVNGIMLSVEKLIKDLKSKEVPEARAYL   750

Lipo  KVHGQEVVFAELDKKMMQRISQLWHSARSHHAAA--QEQIRAVVSKLEQGMDVLLTKGYV   801
ApoB  RILGEELGFASLHDL------------------QLLGKLLLMGARTLQGIPQMIGEVIR   791

Lipo  VSEVR--YMQPVCIGIPMDLNLLVSGVTTNRANLHASFSQSLPADMKLADLLATNIELRV   859
ApoB  KGSKNDFFLHYIFMENAFELPTGAGLQLQISSSGVIA-----PGAKAGVKLEVANMQAEL   846

Lipo  AATTSMSQHAVAIMGLTT-DLAKAGMQTHYKTSAGLGVNGKIEMNARESNFKASLKPFQQ   918
ApoB  VAKPSVSVEFVTNMGIIIPDFARSGVQMNTNFFHESGLEAHVALKAGKLKF---IIPSPK   903

Lipo  KTVVVLSTMESIVFVRDPSGSRILPVLPPKMTLDKGLISQQQQQPHHQQQPHQHGQDQAR   978
ApoB  RPVKLLSGGNTLHLVSTTKTEVIPPLIENR-----------------------------   933

Lipo  AAYQRPWASHEFSPAEQKQIHDIMTARPVMRRKQHCSKSAALSSKVCFSARLRNAAFIRN  1038
ApoB  ----------------------------QSWSVCKQVFP-GLNYCTSGAYSNASSTDS   962

Lipo  ALLYKITGDYVSKVYVQPTSSKAQIQK-VELELQAGPQ                        1075
ApoB  ASYYPLTGDTRLELELRPTGEIEQYSVSATYELQREDR                        1000
```

FIGURE 2 Alignment over the first 1000 residues of apoB. The complete alignment was used to make the apoB1000 model. The first 620 residues of the alignment were taken from Fig. 1 *A*. The alignment from 621–1000 was done using the results from the MACAW and LOCATE analyses (Fig. 1, *B* and *C*). The text highlighted in red represents residues not resolved in the lipovitellin crystal structure.

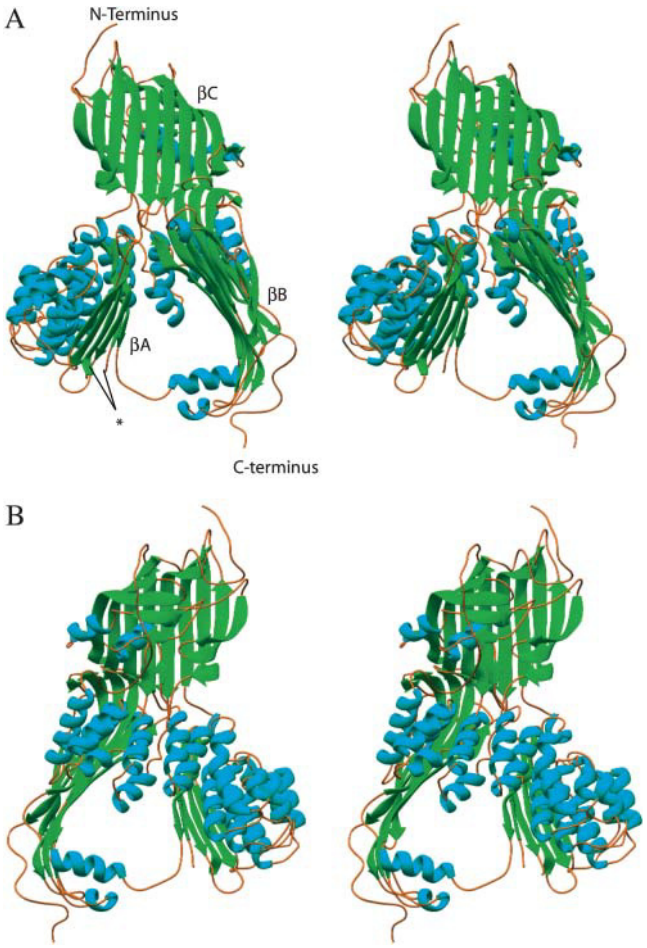

FIGURE 3 ApoB-1000. (*A*) RIBBONS diagram of the apoB1000 model looking from the large opening of the β-sheets toward the small opening. (*B*) RIBBONS diagram of the apoB1000 model looking from the small opening of the β-sheets (180° rotation from Fig. 4 *A*). Residues 670–745 are not shown, but the asterisk symbol (*) in *A* (*left diagram*) indicates where the loop would be inserted.

results indicate that the cysteines are in close enough proximity to the correct partners so that a disulfide bond could form. What makes this significant is that only two disulfide bonds in the model of apoB:1000 are homologous (based on sequence analysis) to those found in the lipovitellins (Table 2). The remaining five disulfide bonds did not have homologous matches in the lipovitellins, but the location of the cysteines in the model allowed them to be in the correct proximity of their corresponding partners to form disulfide bonds (Fig. 4). In particular, the disulfide bond Cys^{939}•Cys^{949} is located near the end of the sequence and links adjacent β-strands in the βB-sheet. In sum, these results are a strong indication of the validity of our apoB:1000 model.

Prolines

The sequence alignment is critical for the correctness of the homology model, since the model is based on alignment to the

TABLE 2 HOMOLOGY TO DISULFIDE BONDS

Disulfide pair	Position	Homologous in ApoBs	Homologous in lipovitellins
1	12	M, L	
2	51	M, R, L	S, F
1	61	M, R, L	
2	70	M, R, L	
3	159	M, R, L	L, C, S, F, T, Tr, K
3	185	M, R, L	L, C, S, F, T, Tr, K
4	218	M, R, L	
4	234	M, R, L	
5	358	M, R, L	
5	363	M, R, L	F
6	451	M, R, L	
6	486	M, R, L	
7	939	M, R, L	L, C, S, F, Tr, K
7	949	M, R, L	L, C, S, F, Tr, K

M, Mouse apoB; *L*, lamprey lipovitellin; *R*, Rabbit apoB; *C*, Chicken lipovitellin; *L*, Lemur apoB; *S*, Sturgeon lipovitellin; *F*, Frog lipovitellin; *T*, Talipia lipovitellin; *Tr*, Trout lipovitellin; and *K*, Killifish lipovitellin. Comparison of Cys positions of human apoB to apoBs and lipovitellins. The disulfide pair number is a list of Cys pairs in the disulfide. The position reflects the residue number in human apoB and the remaining two columns lists homologous Cys in apoBs and/or lipovitellins.

crystal structure. The placements of the proline residues are highly conserved in apoB for human, mouse, rabbit, and lemur (data not shown). In the human apoB:1000 sequence, 42 of 51 prolines are absolutely conserved between these four apoB sequences. Only two prolines in the human sequence are unique, with no homologous matches, whereas the remaining seven prolines are conserved in at least one of the other apoBs. Comparisons of the apoBs to the lipovitellins show that, through residues 1–600, only a few prolines are conserved. A

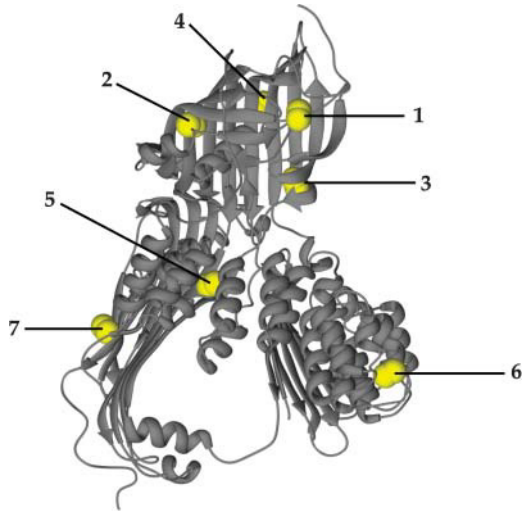

FIGURE 4 Disulfides in ApoB-1000. Stereo view of ApoB-1000 from the small opening side. Cysteines are highlighted by spacefill and the sulfur is colored yellow: (*1*) 12Cys:61Cys; (*2*) 51Cys:70Cys; (*3*) 159Cys:185Cys; (*4*) 218Cys:234Cys; (*5*) 358Cys:363Cys; (*6*) 451Cys:486Cys; and (*7*) 939Cys:949Cys.

higher degree of conservation of proline positioning is noted in the β-sheet regions of the model (residues 619–1000). This is highlighted in the βB-sheet of apoB (Fig. 5). In the first 780 residues of the model (excusive of the βB-sheet), the prolines are located in the expected positions: at loops and at the beginning or end of strands and helices, and occasionally within helices, where they can adopt a conformation that bends the helix yet still allows the helix to continue.

In the βB-sheet region of the model, 7 out of 12 prolines are conserved in mouse, human, rabbit, and lemur apoB. One out of the 12 is conserved in the apoBs and one lipovitellin and one proline was conserved in all four apoBs and three of the lipovitellins (Fig. 5). Only one proline is unique to human apoB and it is located at the apex of a short turn in the model. Most of the prolines in the βB-sheet are located in loops or at the beginning or ending of strands of helices, except one highly conserved proline in the middle of a β-strand (Pro^{850}). It is possible to have a proline in a β-strand because the expected ϕ,ψ-angles of prolines do overlap in a small region of expected β-structures (Richardson and Richardson, 1990). Prolines are sometimes found in β-sheets, located at the beginning/ending of strands or at the edge of a sheet.

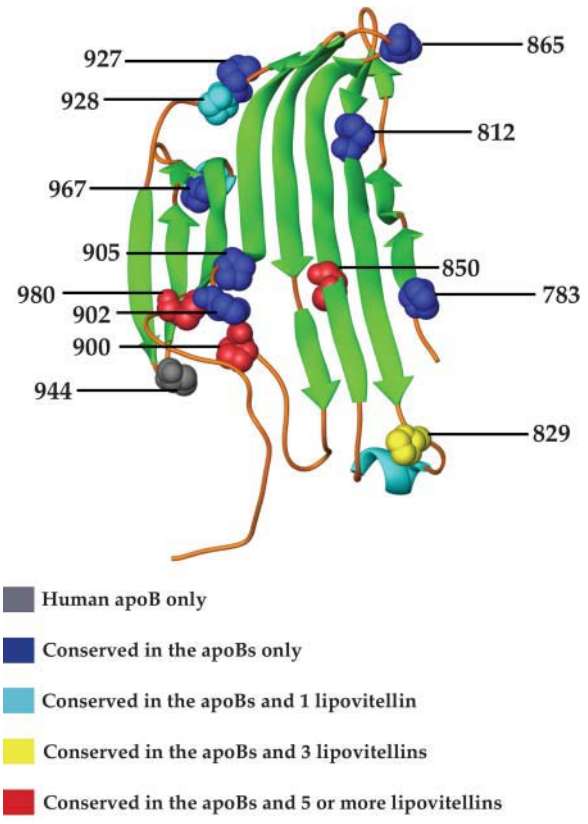

FIGURE 5 Proline punctuation and conservation in the βB-sheet. Prolines are represented in the spacefilling mode and colored based on conservation. Homology based on MACAW alignments among human apoB, mouse apoB, lemur apoB, rabbit apoB, lamprey lipovitellin, chicken lipovitellin, frog lipovitellin, trout lipovitellin, talipia lipovitellin, killifish lipovitellin, and sturgeon lipovitellin.

The residue Pro^{850} is not conserved in the lipovitellin crystal structure, but homologous matches were found in mouse, rabbit, and lemur apoB and frog, tilapia, killifish, trout, and sturgeon lipovitellin. We believe that the placement of the prolines to be correct, because seven of these (P783, P850, P900, P902, P905, P944, and P980) form a row that runs perpendicular to the direction of the strands in the βB-sheet. A portion of this row corresponds to the position of the pronounced fold in the βB-sheet in lamprey lipovitellin; four of the seven prolines are located in this fold in human apoB, suggesting that the βB-sheet in apoB may have a fold across most of its width. The high degree of conservation of the prolines in mammalian apoBs (human, mouse, lemur, and rabbit) in the βB-sheet and their conserved positions in the lipovitellins further support the alignment used to create the model.

Conservation of β-sheet hydrophobicity

The surface of the βA-sheet facing into the proposed lipid pocket is almost uniformly hydrophobic (Fig. 6 *A*). The only charged residues found in this sheet are located at the edges of the pocket and are presumably associated with the surrounding solvent, not the hydrophobic interior of the lipid pocket. The interior surface of the βB-sheet is also quite hydrophobic (Fig. 6 *B*), but contains substantial differences from the comparable face of the βA. Whereas the βA has only a few charges at the base of the sheet, βB has charges that surround three sides of the sheet, including a high density of positive charges at its base (the end opposite the α-helical domain). As already noted, the βB-sheet is also unique in that there is a central bulge caused by a row of prolines (Fig. 5) that extends perpendicular to the direction of the individual β-strands of the sheet. This bulge creates a small opening in the sheet that contains a Lysine and Aspartic acid at its apex, residues that close most of the opening.

The molecular model for the $\beta\alpha_1$-domain of apoB shown in Fig. 3 is therefore almost certainly correct in its general features. The strongly amphipathic β-sheet polarity of the βA- and βB-domains from lipovitellin has been preserved in apoB. These sheets are held in place by their association with the interior portion of the double-layered α-helical bundles. Small regions of hydrophobic and hydrophilic patches on both the βA- and βB-sheets (exterior facing the helices) and the helical bundle match up to allow sheet-helix association. This is additional evidence for the correctness of the model.

DISCUSSION

We have used detailed sequence analysis and the crystal structure of silver lamprey lipovitellin to model residues 1–1000 of human apoB. Mann and co-workers used a global sequence alignment (ClustalW), and they modeled the first 587 residues of apoB (Mann et al., 1999). This allowed them to do a detailed analysis on the MTP:apoB interaction, but

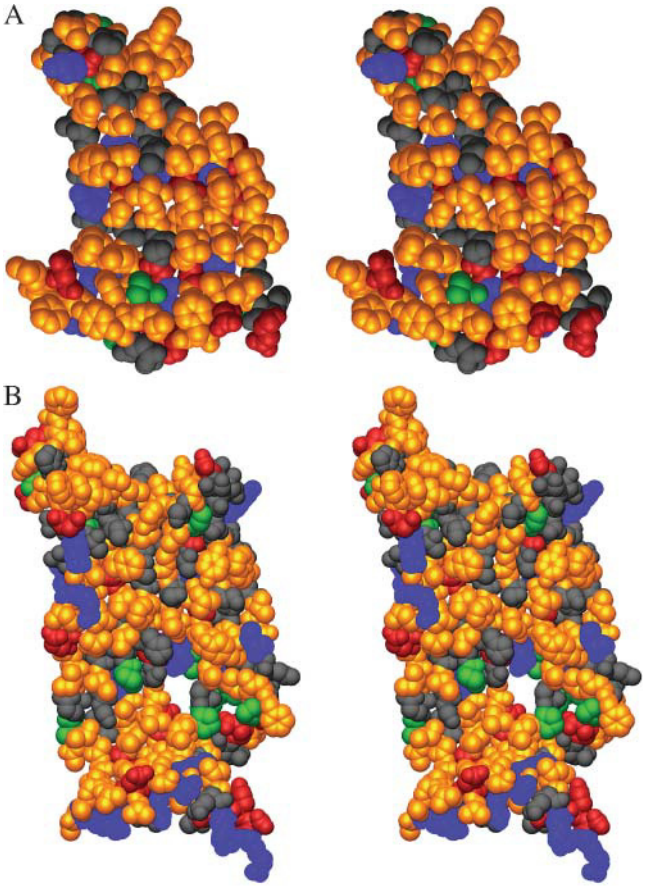

FIGURE 6 Hydrophobicity of the βA- and βB-sheets. Stereo diagrams of the βA-sheet (*A*) and the βB-sheet (*B*). The faces shown are those that are exposed to the interior of the opening between the βA- and βB-sheets. Hydrophobic residues are colored gold, acidic residues are red, basic residues are blue, prolines are green, and polar residues not belonging to any of the group above are gray.

the model did not offer insight into the lipid-binding domain of apoB. We were able to produce an alignment over the first 1000 residues that had similarity and identity alignment scores similar to that of the Mann model.

Both models also contain the critical D524-R531-E557 buried salt-bridge in identical positions. This salt-bridge was identified as homologous in MTP and lipovitellins and proposed as an important structural feature for stabilizing the protein structure in the α-helical region (Mann et al., 1999). Mutations at these key residues cause the proteins to lose solubility and unfold (Mann et al., 1999).

Recent proteoglycan-binding experiments are also consistent with our model. It has been proposed that residues 84–94 of apoB are the principal proteoglycan binding sites in chylomicrons and LDL (Flood et al., 2002; Goldberg et al., 1998). This region is located at an exposed loop that sits at the base of the βC-domain (β-barrel) in our model. There are three lysines in this location that could potentially bind to proteoglycan.

The model shown in Fig. 3 is incomplete, since the third side of the pyramidal hydrophobic cavity required to create an effective lipid pocket like that possessed by lipovitellin is missing. It was for this reason that we originally suggested that MTP might create the third side (Segrest et al., 1999). However, further analysis of the apoB:1000 model suggests an alternate possibility for the structural nature of the third side to the pocket. A tandem series of four charged residues (Arg^{997}, Glu^{998}, Asp^{999}, and Arg^{1000}) is located at the C-terminal end of the model and forms a portion of the base of the βB-sheet. On further analysis of the apoB:1000 sequence, a complementary tandem series of four charges (Glu^{720}, His^{719}, Lys^{718}, Asp^{717}) was found in the unmodeled loop region (670–745) located in the middle of the βA-sheet. LOCATE analysis of residues 670–745 showed the presence of two well-defined amphipathic helices $AH_{702–716}$ and $AH_{721–738}$, predicted to be strongly lipid-associating. Significantly, the complementary tandem charges are located precisely between the two putative amphipathic helices, suggesting a helix-turn-helix motif.

We have built a helix-turn-helix model of residues 700–744 using the LOCATE analysis as a guide. The helix-turn-helix model was incorporated into the apoB model to create a partially closed lipid pocket (Fig. 7 *A*). This hairpin-bridge spans the third side of the pyramidal lipid pocket allowing the charged residues in the turn region to form complementary salt-bridges with the charged residues in the C-terminal portion of the βB-sheet. The hydrophobic faces of the helices orient toward the lipid-binding pocket (Fig. 7 *B*). Four salt-bridges can be formed from this arrangement: Arg^{997}—Glu^{720}, Glu^{998}—His^{719}, Asp^{999}—Lys^{718}, and Arg^{1000}—Asp^{717} (Fig. 7 *C*). We propose that the salt-bridges serve as a lock to close the third side of the asymmetric pyramidal lipid pocket by the creation of a hairpin-bridge that completes the nascent step of lipoprotein particle assembly.

It seems probable that the lipids would form a bilayerlike assembly in the nascent lipid pocket. This conclusion is based upon the depth of the pocket (~40 Å) similar to the thickness of the hydrophobic core of a phospholipid bilayer and the strong tendency of phospholipids to assemble as bilayers. In such an assembly, the charged headgroups of the phospholipids would be located at the basal and apical openings of the lipid pocket, associating with the charges at the edges of the β-sheets; the fatty acyl chains of the phospholipids would be directed into the hydrophobic cavity formed by the βA- and βB-sheets.

We have manually docked 48 POPC molecules into the lipid pocket of the apoB:1000 model to create an asymmetric bilayer with 14 POPC in the apical monolayer and 34 POPC in the basal monolayer (Fig. 8). A few more POPC molecules could be docked into the pocket if the bilayer surfaces were allowed to curve and more sophisticated methods, such as energy minimization and molecular dynamics, were used in creating the model. Experimentally apoB:1000 is secreted in the form of a lipoprotein particle, containing ~50

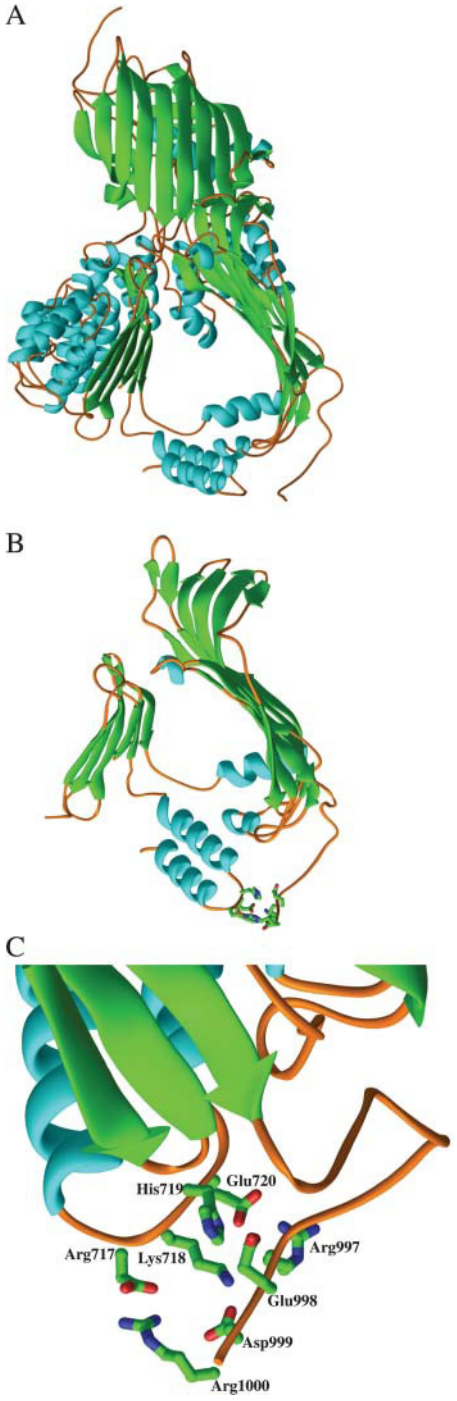

FIGURE 7 Lipid pocket. (*A*) RIBBONS diagram of the apoB1000 model, including the modeled helix-loop-helix region (700–744). (*B*) Ribbons diagram of the proposed lipid pocket domain of the apoB1000 model, including the modeled helix-loop-helix. The critical residues responsible for the salt-bridges are represented in an all-atom detail as tubes. (*C*) Ribbons diagram of a closeup of the region responsible for the lock that stabilizes the helix-loop-helix. The critical residues are shown as tubes, and the salt-bridges are represented as solid lines.

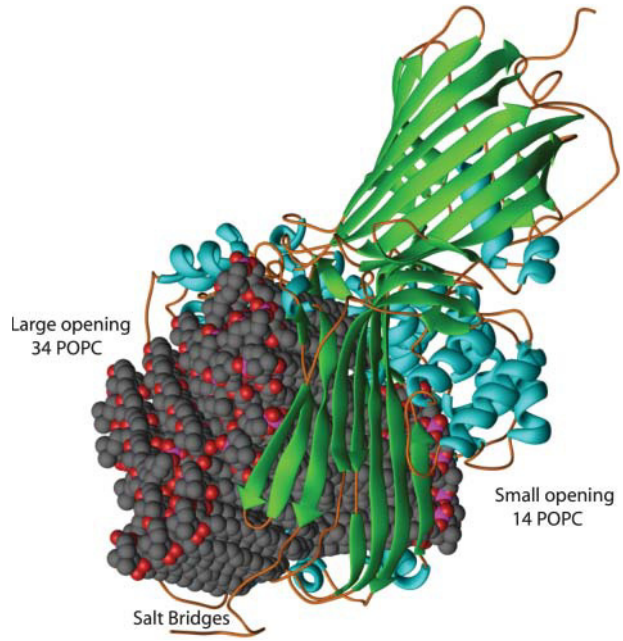

FIGURE 8 The lipid pocket. ApoB-22.5 is represented with β-strands shown as yellow arrows and α-helices shown as purple tubes. POPC is shown as spacefill rendering with carbons in gray and oxygen in red. There are 34 POPC in the large opening and 14 POPC in the small opening, for a total of 48 POPC fit into the lipid pocket of ApoB-22.5.

phospholipids per particle (Manchekar et al., 2004), which is an excellent fit to our model.

We believe that the hairpin-bridge is a transient intermediate in lipoprotein assembly with two distinct forms: a locked hairpin-bridge that closes the pocket to allow the formation of a nascent lipoprotein particle with defined lipid content, and an unlocked form that allows an increase in the particle size and decrease in the particle density through addition of lipid.

We previously showed (Dashti et al., 2002) that the major apoB-containing particles formed by B:931 (residues 1–931) have a constant diameter of 110 Å across a wide range of densities and a mean density of 1.25 g/ml or greater; therefore, this particle contains little lipid and is considerably denser than traditional HDL, which has density in the range of 1.063–1.21 g/ml (Dashti et al., 2002). The major apoB-containing particle formed by B:1000 has a diameter that remains constant at ~112 Å across a wide range of densities and a mean density of 1.21 g/ml that is within the HDL_3 density range of 1.125–1.21 g/ml (Dashti et al., 2002). Thus over a short stretch of 69 residues from apoB:931 to apoB:1000, the nature of the secreted particles changes from lipid-poor to an HDL-like particle (Fig. 9). This was confirmed by incorporation of [^{14}C]-labeled oleic acid into the lipid fraction of the particles, determined by autoradiography and densitometry, showing a 10-fold increase in the lipid content of apoB:1000-containing particles relative to those reconstituted with apoB:931. Finally, the larger apoB:1200 particle has

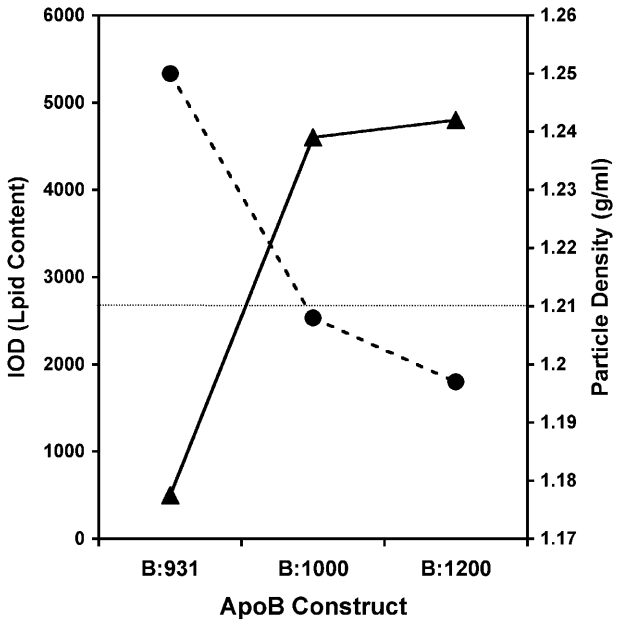

FIGURE 9 Density and lipid content of truncated apoB-containing particles. McA-RH7777 cells were incubated for 24 h in serum-free DMEM containing 0.4 mM of unlabeled or [^{14}C]-labeled oleic acid bound to 0.75% BSA. Unlabeled conditioned medium was analyzed for the peak density and [^{14}C]-labeled conditioned medium was analyzed for the radioactive lipid content of truncated apoB-containing particles, as described in Materials and Methods. Solid circles represent the densities of the major particles produced by B-20.5, B-22.5, and B-26.5. The solid triangles represent the [^{14}C]-labeled lipid content of these particles determined by autoradiography and densitometry.

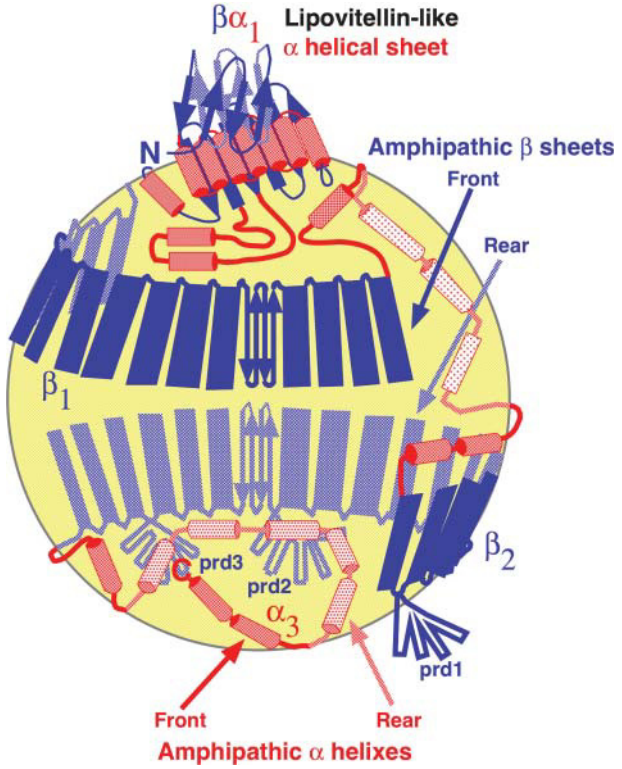

FIGURE 10 Open form of the pocket. Cartoon representation of apoB-100 on the LDL particle. The first 1000 residues are shown in detail (*top* of the *particle*), whereas the remaining residues are represented as a cartoon rendering based on the proposed pentapartite model for apoB-100. Blue boxes represent amphipathic β-strands and red cylinders represent amphipathic helices. PRD2 and PRD3 show the location of the proline-rich domains in the model.

a diameter that increased with decreasing density, ranging from 118 to 127 Å, and a mean density of 1.197 g/ml that is within the HDL density range, clearly indicating that the apoB:1200 particle contains additional, but varying, lipid compared to the apoB:1000 particle.

These results suggest the following model: The lipid pocket created upon formation of B:1000 is involved co-translationally in the preliminary acquisition of phospholipids and triglycerides to form a nascent lipoprotein particle. Beyond residue 1000 lies the β_1-domain containing multiple amphipathic β-strands. Translation of these structural motifs provides a mechanism for lipoprotein particle growth beyond the nascent apoB:1000 particle. Co-translation of the amphipathic β-sheets of the β_1-domain beyond residue 1000 tightly couple with accumulation of additional lipid molecules in the pocket, inducing opening of the hairpin-bridge. To create a stable particle, the hairpin-bridge opening would have to occur simultaneously with addition of multiple amphipathic β-strands to the lipoprotein particle surface to form stabilizing amphipathic β-sheets. As the lipid pocket expands, lipids would be added to the flexible basal opening of the lipid pocket, to create what is, in effect, an expanding lipid droplet. Residues 764–779 would serve as the pivot point for the pocket opening and separation of the βA- and βB-sheets at the basal end (Fig. 10). The hairpin-bridge would unlock and open the base of the pocket, and the amphipathic helices of the helix-turn-helix would associate with the growing particle. Ultimately this would cause the V-shaped pocket between βA- and βB-sheets to open. The open conformation would easily associate with the surface of a spheroidal particle that is much larger in size than that of the B:1000 domain of the protein itself. We suggest that this would be the conformation of apoB bound to LDL, intermediate-density lipoprotein, and chylomicrons.

Our hairpin-bridge lipid pocket model suggests that apoB:1000 can assemble lipid, presumably delivered by MTP acting as a shuttle, to form a nascent lipoprotein particle without requiring MTP to also serve as an integral structural element of the lipid pocket. It has been shown (Manchekar et al. 2004) that apoB:1000 forms stable particles without the 1:1 ratio of apoB to MTP required if MTP were serving as a structural member of the lipid pocket. These results together show that, compatible with our hairpin-bridge pocket closure mechanism, MTP is not required to function as a structural element necessary for assembly of a lipoprotein particle.

Spin and Atkinson reported images of LDL in vitreous ice using electron cryomicroscopy at ~30 Å resolution (Spin and

Atkinson, 1995). In their study, LDL appeared to be a quasispherical particle, ~220–240 Å in diameter, with a region of low density surrounded by a ring of high density (in projection) believed to represent apoB-100. Some images were egg-shaped and contained a pointed end; the pointed end had the approximate dimensions of the β-barrel in Fig. 10 and subsequently has been shown to represent the N-terminal globular region (the $\beta\alpha_1$-domain) of apoB (D. Atkinson, personal communication).

One difficulty for making a model of apoB is the complexity and expandability of the protein. ApoB is a very dynamic protein that undergoes expansion and contraction as the lipid particle changes sizes, and this will inherently change the overall structure and secondary structure of the protein. Certain regions of the model lack secondary structure where analysis of the sequence suggests that secondary structure might be present. A region of particular importance is the sequence 670–701 N-terminal to the modeled helix-turn-helix (700–744). Since the sequence homology is very low for this region so we decided not to include it in the model. LOCATE analysis of this region (670–699) showed the presence of one significant amphipathic α-helix (672–680). We therefore believe that the sequence 670–699 serves, in some as yet undefined conformation, to close the gap present at the base of the triangular pocket formed by the hairpin-bridge with βA and βB.

Yet another area where the model might not reflect the structure is at the C-terminus of the apoB model (986–995). A unique characteristic of this region is alternating hydrophobic and hydrophilic residues (**QYSVSATYEL**), suggesting that this region is an amphipathic β-strand. It is also likely that region 895–900 is a strand, and that the two strands are hydrogen-bonded together to form a small sheet (model not shown). Changing these resides to the more defined secondary structure of a β-sheet would close the second gap present in the model at the base of the triangular pocket, which would cover the remaining exposed lipids.

The model suggests an answer to the question of how triglycerides and cholesterol esters get into and out of lipid particles. The β-barrel (βC) has a hydrophobic interior that could bind lipids, as in the crystal structure of lipovitellin, where a lipid has been resolved in the barrel region (Raag et al., 1988; Sharrock et al., 1992). If there were an opening between the β-barrel and the lipid pocket, this could provide a channel through which triglycerides and cholesterol esters could move. There is no such opening in our model, which represents the conformation of apoB bound to only a handful of lipids, because the bottom of the β-barrel is partially blocked by the βA- and βB-sheets. In the mature particle, however, the pocket formed by the βA- and βB-sheets must be opened to fit the lipid surface of the mature LDL. We have examined the effects of widening the large opening of the pocket, expanding the pocket by 10 Å (data not shown) using the modeling package INSIGHT2. These motions are sufficient to open a channel between the β-barrel and the lipid pocket. If this extension of our model is correct, then the β-barrel would be the portal through which triglycerides and cholesterol esters might move into the lipid particle as it grows. These molecules presumably accumulate between the leaflets of the bilayer in the lipid pocket initially. Although the exact shape of the lipid particle during this accumulation is unclear, it would not be difficult to modify the lipid bilayer in our model to accommodate triglycerides and cholesterol esters. In the mature lipid particle, these molecules would be transferred into or out of the interior of the particle through the β-barrel.

The evidence from the sequence alignments (cysteine positioning for disulfide bond formation, proline positioning, and conservation of the hydrophobic faces of the amphipathic βA-and βB-sheets), proteoglycan binding site experiments, and the experimental data about the quantity of lipids in the secreted apoB:1000 lipoprotein particle, all indicate that the model is correct in its general structure. The model suggests that there is a multitude of structural changes that take place from the initial assembly of a nascent lipoprotein particle to the structure of the mature lipid particle.

Supported by National Institutes of Health grants P41 RR12255 (to S.C.H.: C.L. Brooks 3rd, Scripps Research Institute, Principal Investigator) and P01 HL34343 (to J.P.S).

REFERENCES

Altschul, S. F., W. Gish, W. Miller, E. W. Myers, and D. J. Lipman. 1990. Basic local alignment search tool. *J. Mol. Biol.* 215:403–410.

Atkinson, D., R. J. Deckelbaum, D. M. Small, and G. G. Shipley. 1977. Structure of human plasma low-density lipoproteins: molecular organization of the central core. *Proc. Natl. Acad. Sci. USA.* 74:1042–1046.

Baker, M. E. 1988. Is vitellogenin an ancestor of apolipoprotein B-100 of human low-density lipoprotein and human lipoprotein lipase? *Biochem. J.* 255:1057–1060.

Carson, M. 1991. Ribbons 2.0. *J. Appl. Crystallogr.* 24:958–961.

Chatterton, J. E., M. L. Phillips, L. K. Curtiss, R. Milne, J. C. Fruchart, and V. N. Schumaker. 1995a. Immunoelectron microscopy of low density lipoproteins yields a ribbon and bow model for the conformation of apolipoprotein B on the lipoprotein surface. *J. Lipid Res.* 36:2027–2037.

Chatterton, J. E., M. L. Phillips, L. K. Curtiss, R. W. Milne, Y. L. Marcel, and V. N. Schumaker. 1991. Mapping apolipoprotein B on the low density lipoprotein surface by immunoelectron microscopy. *J. Biol. Chem.* 266:5955–5962.

Chatterton, J. E., P. Schlapfer, E. Butler, M. M. Gutierrez, D. L. Puppione, C. R. Pullinger, J. P. Kane, L. K. Curtiss, and V. N. Schumaker. 1995b. Identification of apolipoprotein B100 polymorphisms that affect low-density lipoprotein metabolism: description of a new approach involving monoclonal antibodies and dynamic light scattering. *Biochemistry.* 34: 9571–9580.

Chen, S. H., G. Habib, C. Y. Yang, Z. W. Gu, B. R. Lee, S. A. Weng, S. R. Silberman, S. J. Cai, J. P. Deslypere, and M. Rosseneu. 1987. Apolipoprotein B-48 is the product of a messenger RNA with an organ-specific in-frame stop codon. *Science.* 238:363–366.

Dashti, N., M. Gandhi, X. Liu, X. Lin, and J. P. Segrest. 2002. The N-terminal 1000 residues of apolipoprotein B associate with microsomal triglyceride transfer protein to create a lipid transfer pocket required for lipoprotein assembly. *Biochemistry.* 41:6978–6987.

Deckelbaum, R. J., G. G. Shipley, and D. M. Small. 1977. Structure and interactions of lipids in human plasma low density lipoproteins. *J. Biol. Chem.* 252:744–754.

Deckelbaum, R. J., G. G. Shipley, D. M. Small, R. S. Lees, and P. K. George. 1975. Thermal transitions in human plasma low density lipoproteins. *Science.* 190:392–394.

Du, E. Z., S. L. Wang, H. J. Kayden, R. Sokol, L. K. Curtiss, and R. A. Davis. 1996. Translocation of apolipoprotein B across the endoplasmic reticulum is blocked in abetalipoproteinemia. *J. Lipid Res.* 37:1309–1315.

Flood, C., M. Gustafsson, P. E. Richardson, S. C. Harvey, J. P. Segrest, and J. Boren. 2002. Identification of the proteoglycan binding site in apolipoprotein B48. *J. Biol. Chem.* 277:32228–32233.

Gantz, D. L., M. T. Walsh, and D. M. Small. 2000. Morphology of sodium deoxycholate-solubilized apolipoprotein B-100 using negative stain and vitreous ice electron microscopy. *J. Lipid Res.* 41:1464–1472.

Goldberg, I. J., W. D. Wagner, L. Pang, L. Paka, L. K. Curtiss, J. A. DeLozier, G. S. Shelness, C. S. Young, and S. Pillarisetti. 1998. The NH2-terminal region of apolipoprotein B is sufficient for lipoprotein association with glycosaminoglycans. *J. Biol. Chem.* 273:35355–35361.

Greeve, J., N. Navaratnam, and J. Scott. 1991. Characterization of the apolipoprotein B mRNA editing enzyme: no similarity to the proposed mechanism of RNA editing in kinetoplastid protozoa. *Nucleic Acids Res.* 19:3569–3576.

Herscovitz, H., M. Hadzopoulou-Cladaras, M. T. Walsh, C. Cladaras, V. I. Zannis, and D. M. Small. 1991. Expression, secretion, and lipid-binding characterization of the N-terminal 17% of apolipoprotein B. *Proc. Natl. Acad. Sci. USA.* 88:7313–7317.

Laskowski, R. A., M. W. MacArthur, D. S. Moss, and J. M. Thornton. 1993. PROCHECK: a program to check the stereochemical quality of protein structures. *J. Appl. Crystallogr.* 26:283–291.

Law, A., and J. Scott. 1990. A cross-species comparison of the apolipoprotein B domain that binds to the LDL receptor. *J. Lipid Res.* 31:1109–1120.

Linton, M. F., R. V. Farese, Jr., and S. G. Young. 1993. Familial hypobetalipoproteinemia. *J. Lipid Res.* 34:521–541.

Manchekar, M., P. E. Richardson, T. M. Forte, G. Datta, J. P. Segrest, and N. Dashti. 2004. Apolipoprotein B-containing lipoprotein particle assembly: lipid capacity of the nascent lipoprotein particle. *J. Biol. Chem.* 279:39757–39766.

Mann, C. J., T. A. Anderson, J. Read, S. A. Chester, G. B. Harrison, S. Kochl, P. J. Ritchie, P. Bradbury, F. S. Hussain, J. Amey, B. Vanloo, M. Rosseneu, R. Infante, J. M. Hancock, D. G. Levitt, L. J. Banaszak, J. Scott, and C. C. Shoulders. 1999. The structure of vitellogenin provides a molecular model for the assembly and secretion of atherogenic lipoproteins. *J. Mol. Biol.* 285:391–408.

Muller, K., P. Laggner, O. Glatter, and G. Kostner. 1978. The structure of human-plasma low-density lipoprotein B. An x-ray small-angle scattering study. *Eur. J. Biochem.* 82:73–90.

Raag, R., K. Appelt, N. H. Xuong, and L. Banaszak. 1988. Structure of the lamprey yolk lipid-protein complex lipovitellin-phosvitin at 2.8 Å resolution. *J. Mol. Biol.* 200:553–569.

Richardson, J. S., and D. C. Richardson. 1990. Principles and patterns of protein conformation. *In* Prediction of Protein Structure and the Principles of Protein Conformation. G.D. Fasman, editor. Plenum Press, New York. 1–98.

Sali, A., and T. L. Blundell. 1993. Comparative protein modelling by satisfaction of spatial restraints. *J. Mol. Biol.* 234:779–815.

Sayle, R. A., and E. J. Milner-White. 1995. RasMol: biomolecular graphics for all. *Trends Biochem. Sci.* 20:374–376.

Schuler, G. D., S. F. Altschul, and D. J. Lipman. 1991. A workbench for multiple alignment construction and analysis. *Proteins.* 9:180–190.

Schumaker, V. N., M. L. Phillips, and J. E. Chatterton. 1994. Apolipoprotein B and low-density lipoprotein structure: implications for biosynthesis of triglyceride-rich lipoproteins. *Adv. Protein Chem.* 45:205–248.

Segrest, J. P., M. K. Jones, and N. Dashti. 1999. N-terminal domain of apolipoprotein B has structural homology to lipovitellin and microsomal triglyceride transfer protein: a ''lipid pocket'' model for self-assembly of apoB-containing lipoprotein particles. *J. Lipid Res.* 40:1401–1416.

Segrest, J. P., M. K. Jones, H. De Loof, and N. Dashti. 2001. Structure of apolipoprotein B-100 in low density lipoproteins. *J. Lipid Res.* 42:1346–1367.

Segrest, J. P., M. K. Jones, V. K. Mishra, G. M. Anantharamaiah, and D. W. Garber. 1994. apoB-100 has a pentapartite structure composed of three amphipathic α-helical domains alternating with two amphipathic β-strand domains. Detection by the computer program LOCATE. *Arterioscler. Thromb.* 14:1674–1685.

Sharp, D., L. Blinderman, K. A. Combs, B. Kienzle, B. Ricci, K. Wager-Smith, C. M. Gil, C. W. Turck, M. E. Bouma, and D. J. Rader. 1993. Cloning and gene defects in microsomal triglyceride transfer protein associated with abetalipoproteinaemia. *Nature.* 365:65–69.

Sharrock, W. J., T. A. Rosenwasser, J. Gould, J. Knott, D. Hussey, J. I. Gordon, and L. Banaszak. 1992. Sequence of lamprey vitellogenin. Implications for the lipovitellin crystal structure. *J. Mol. Biol.* 226:903–907.

Shoulders, C. C., D. J. Brett, J. D. Bayliss, T. M. Narcisi, A. Jarmuz, T. T. Grantham, P. R. Leoni, S. Bhattacharya, R. J. Pease, and P. M. Cullen. 1993. Abetalipoproteinemia is caused by defects of the gene encoding the 97-kDa subunit of a microsomal triglyceride transfer protein. *Hum. Mol. Genet.* 2:2109–2116.

Shoulders, C. C., T. M. Narcisi, J. Read, A. Chester, D. J. Brett, J. Scott, T. A. Anderson, D. G. Levitt, and L. J. Banaszak. 1994. The abetalipoproteinemia gene is a member of the vitellogenin family and encodes an α-helical domain. *Nat. Struct. Biol.* 1:285–286.

Sniderman, A., S. Shapiro, D. Marpole, B. Skinner, B. Teng, and P. O. Kwiterovich, Jr. 1980. Association of coronary atherosclerosis with hyperapobetalipoproteinemia. *Proc. Natl. Acad. Sci. USA.* 77:604–608.

Spin, J. M., and D. Atkinson. 1995. Cryoelectron microscopy of low density lipoprotein in vitreous ice. *Biophys. J.* 68:2115–2123.

Thompson, J. D., D. G. Higgins, and T. J. Gibson. 1994. CLUSTAL W: improving the sensitivity of progressive multiple sequence alignment through sequence weighting, position-specific gap penalties and weight matrix choice. *Nucleic Acids Res.* 22:4673–4680.

Thompson, J. R., and L. J. Banaszak. 2002. Lipid-protein interactions in lipovitellin. *Biochemistry.* 41:9398–9409.

Tyroler, H. A. 1987. Review of lipid-lowering clinical trials in relation to observational epidemiologic studies. *Circulation.* 76:515–522.

van Antwerpen, R., G. C. Chen, C. R. Pullinger, J. P. Kane, M. LaBelle, R. M. Krauss, C. Luna-Chavez, T. M. Forte, and J. C. Gilkey. 1997. Cryo-electron microscopy of low density lipoprotein and reconstituted discoidal high density lipoprotein: imaging of the apolipoprotein moiety. *J. Lipid Res.* 38:659–669.

van Antwerpen, R., M. La Belle, E. Navratilova, and R. M. Krauss. 1999. Structural heterogeneity of apoB-containing serum lipoproteins visualized using cryo-electron microscopy. *J. Lipid Res.* 40:1827–1836.

Welty, F. K., L. Seman, and F. T. Yen. 1995. Purification of the apolipoprotein B-67-containing low density lipoprotein particle and its affinity for the low density lipoprotein receptor. *J. Lipid Res.* 36:2622–2629.

Wetterau, J. R., M. C. Lin, and H. Jamil. 1997. Microsomal triglyceride transfer protein. *Biochim. Biophys. Acta.* 1345:136–150.

Yang, C. Y., T. W. Kim, S. A. Weng, B. R. Lee, M. L. Yang, and A. M. Gotto, Jr. 1990. Isolation and characterization of sulfhydryl and disulfide peptides of human apolipoprotein B-100. *Proc. Natl. Acad. Sci. USA.* 87:5523–5527.